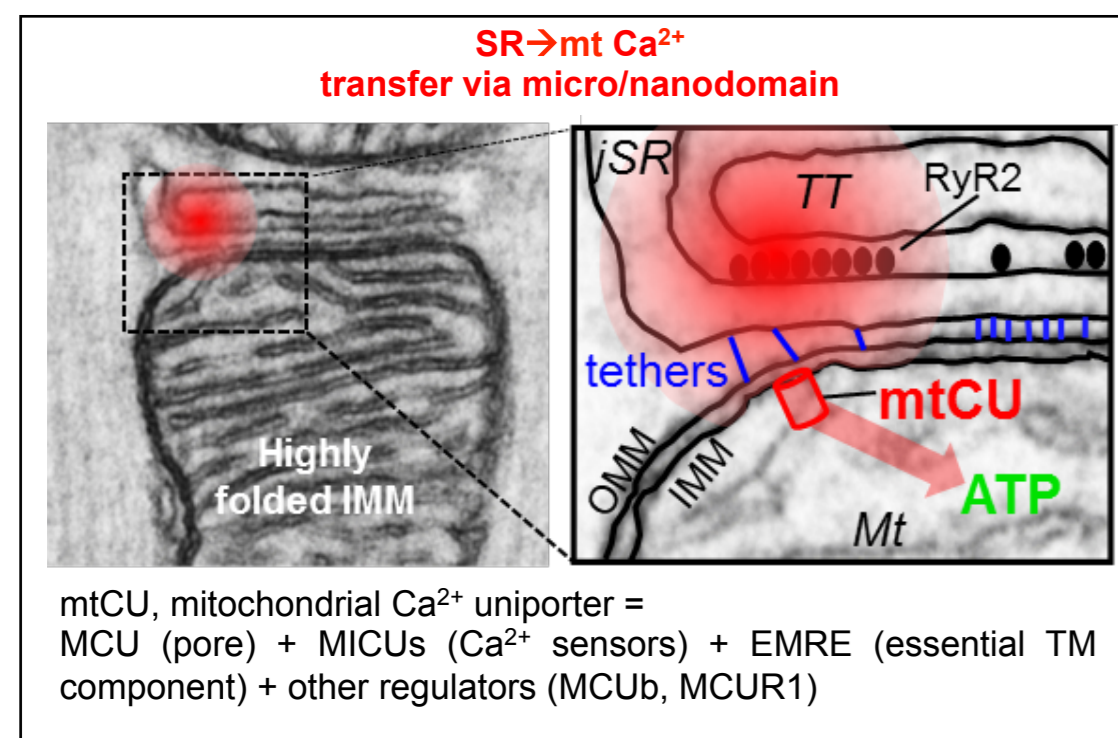


Strategic concentration to mitochondria-SR associations of the mitochondrial Ca^{2+} uniporter: Ca^{2+} uptake hotspots in the cardiac mitochondria

Sergio De La Fuente¹, Caitlin Vail¹, Elorm J. Agra¹, Kira Holmstrom², Junhui Sun³, Jyotsna Mishra⁴, Toren Finkel², Elizabeth Murphy³, Suresh K. Joseph¹, Shey-Shing Sheu⁴, György Csordás¹

¹MitoCare Center, Pathology, Anatomy & Cell Biology, Thomas Jefferson University, Philadelphia, PA, USA, ²Center for Molecular Medicine, Lab. of Molecular Biology, NIH-NHLBI, Bethesda, MD, USA, ³Systems Biology Center, Laboratory of Cardiac Physiology, NIH-NHLBI, Bethesda, MD, USA, ⁴Center for Translational Medicine, Thomas Jefferson University, Philadelphia, PA, USA

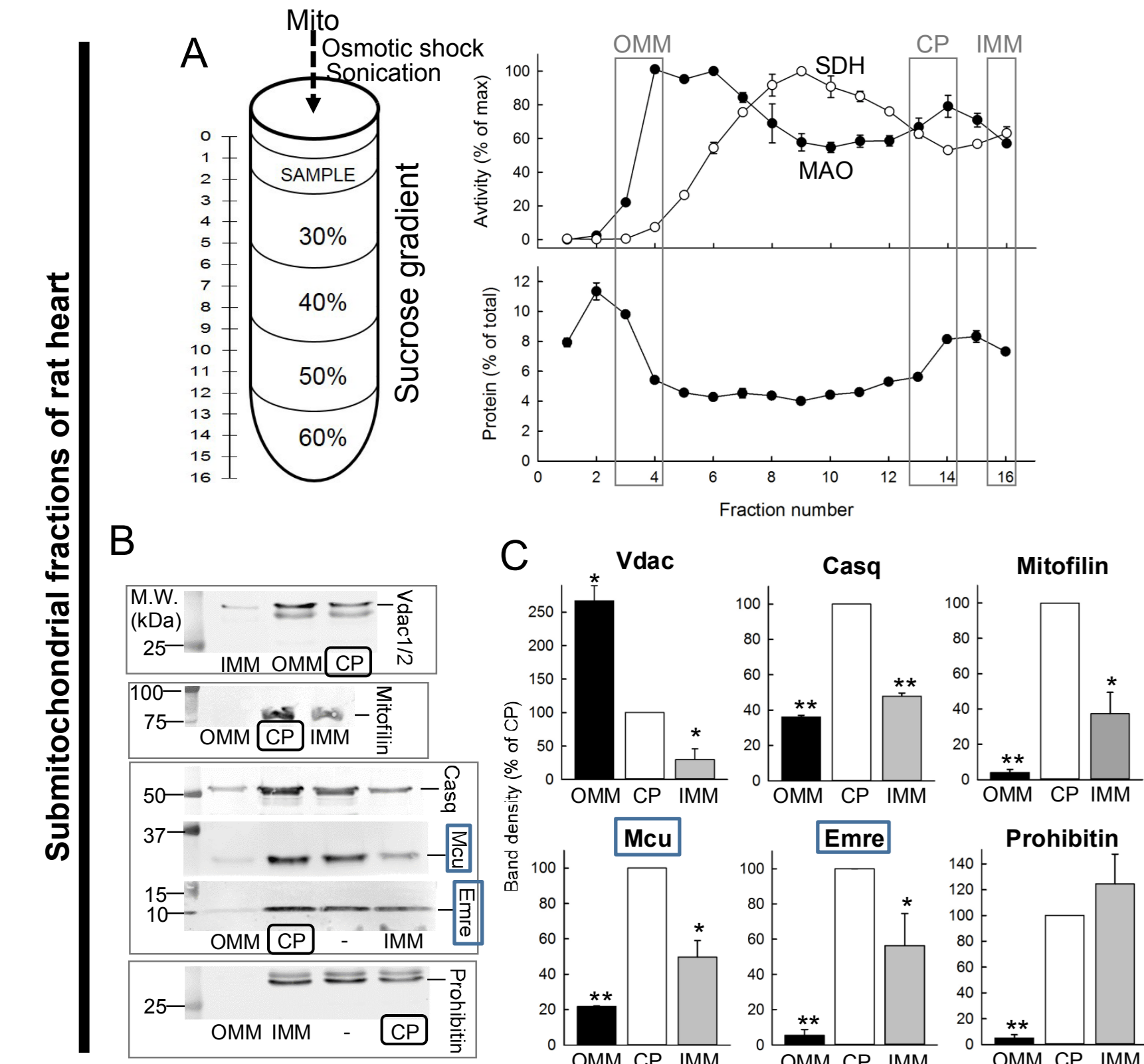
INTRODUCTION



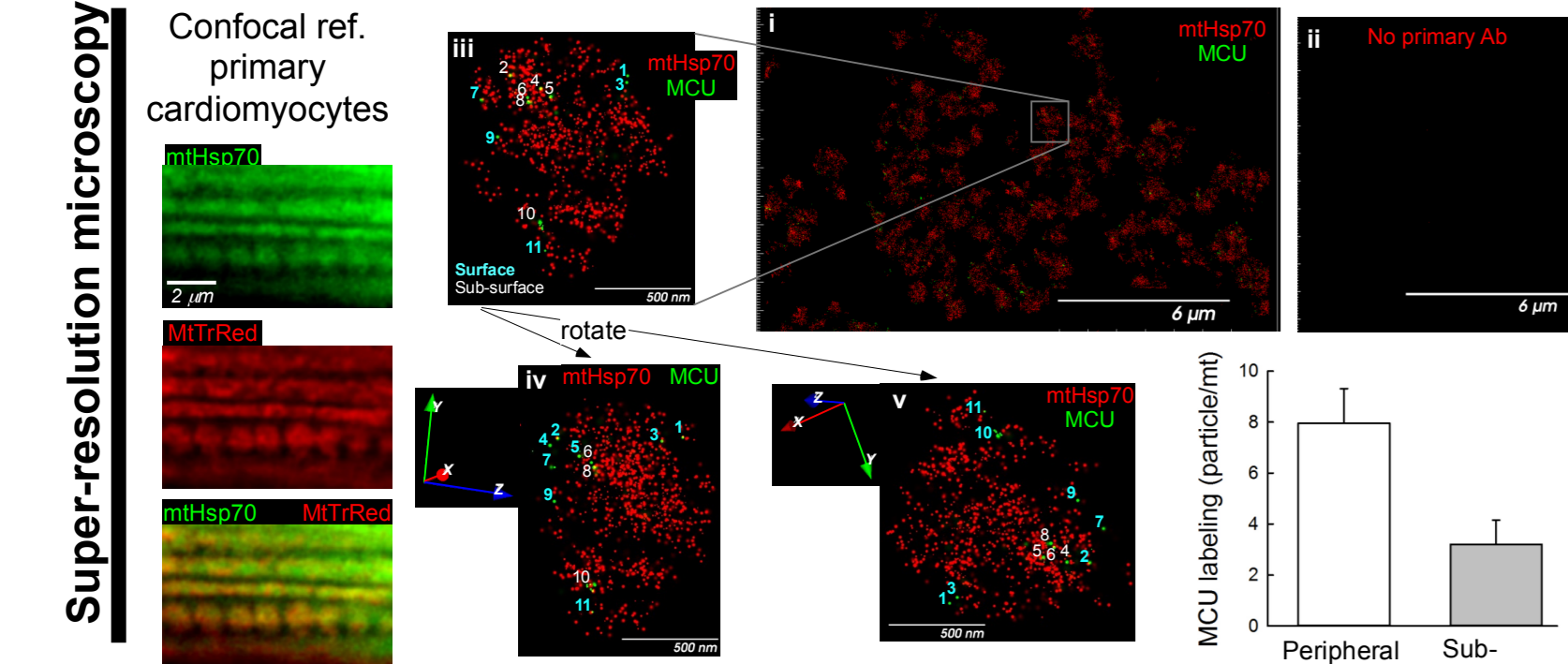
- Control of the mitochondrial ATP production by SR-derived Ca^{2+} signals includes local, nanodomain Ca^{2+} transfer from ryanodine receptors (RyR2) to the mitochondrial matrix (excitation-bioenergetics coupling).
- Ca^{2+} crosses the inner mitochondrial membrane (IMM) via the mtCU, a low-affinity Ca^{2+} -activated Ca^{2+} channel complex.
- The surface area of cardiac IMM is extensively enhanced by cristae folding; however, mitoplast patch clamp studies showed mtCU current density the lowest amongst a range of tissues (Fieni 2012. *Nat Commun*).

Here we tested the hypothesis that mtCU distribution is strategically biased towards mito-SR associations in the heart to support effective excitation-bioenergetics coupling.

1. MCU and EMRE are enriched in the mitochondrial contact points.

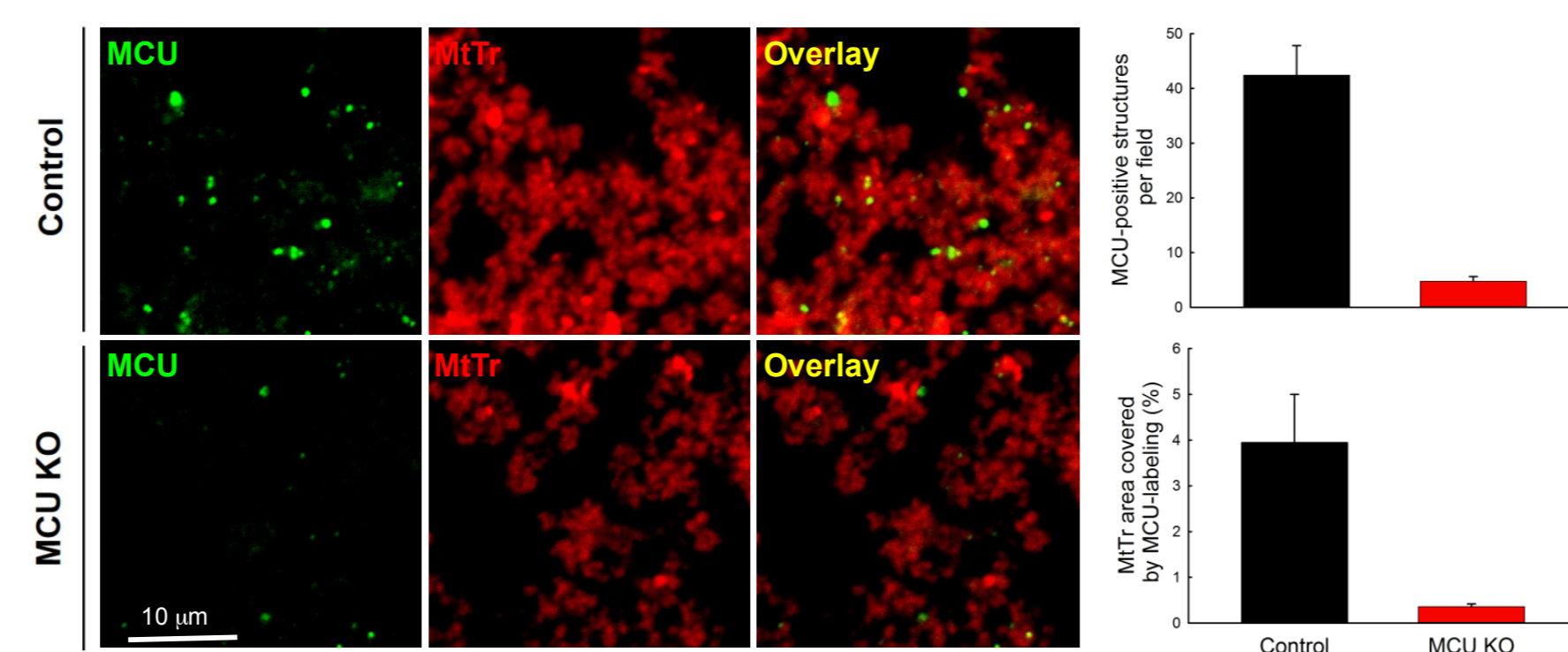


MCU locates to the periphery of the matrix volume



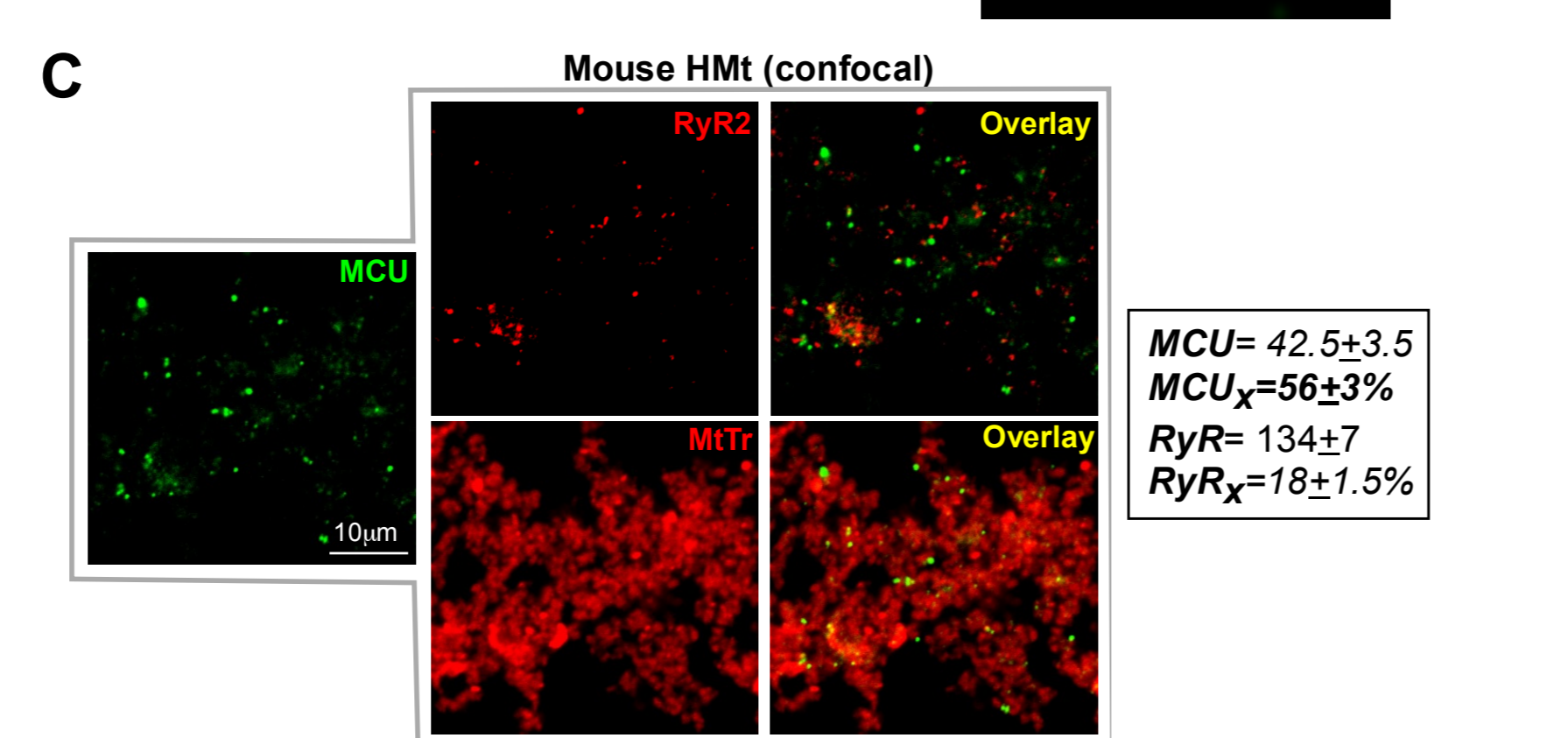
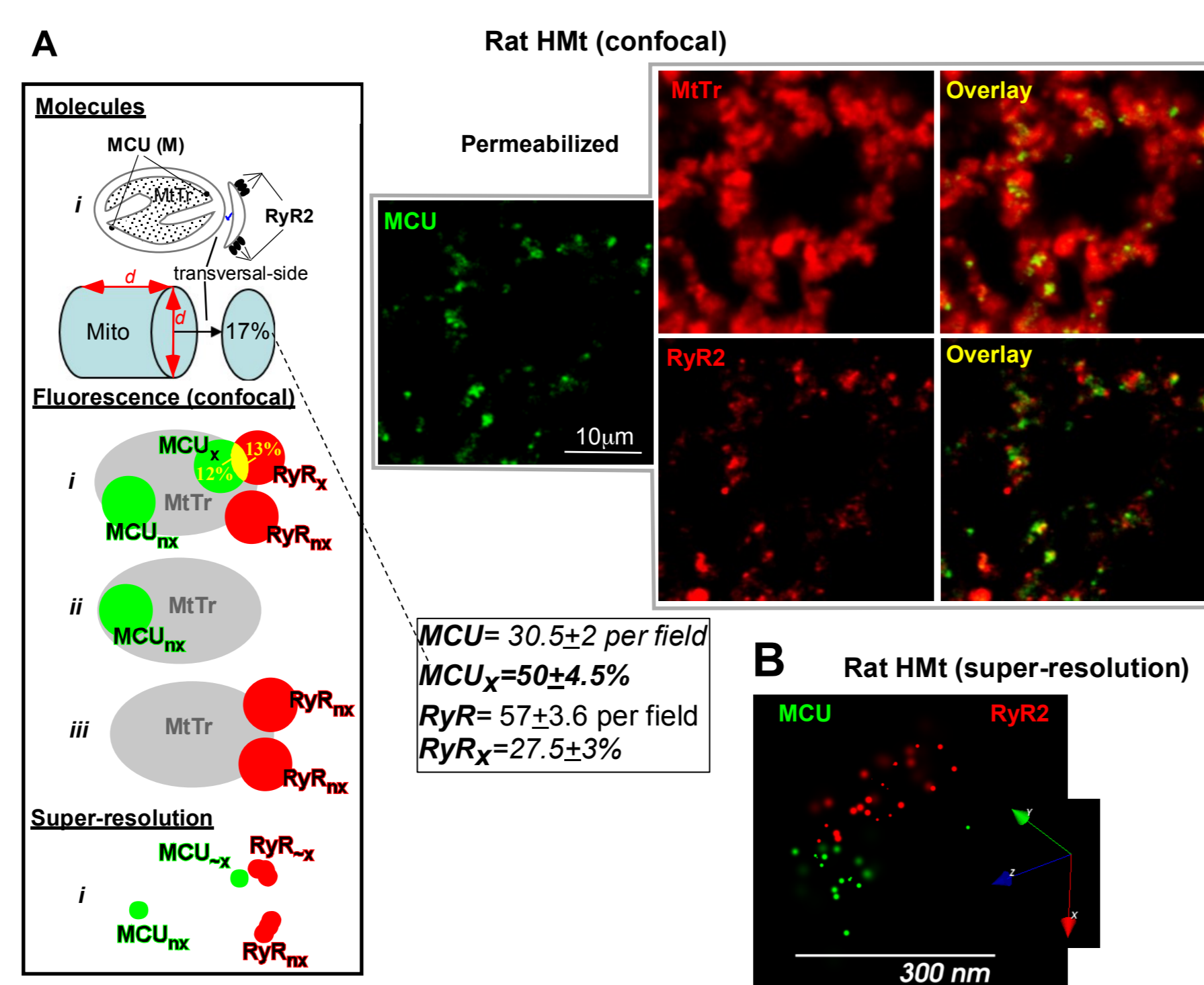
A. Enzyme profiles of MAO (OMM) and SDH (IMM) and protein profile. Three fractions were examined from the 2 protein peaks: OMM, high MAO and no/very low SDH activities; CP, contact points \rightarrow highest MAO activity from the second protein peak (with high SDH); IMM, lowest MAO activity in the second protein peak. **B.** WBs of the indicated mitochondrial and SR proteins. **C.** Relative abundance of mitochondrial and mito-associated SR proteins normalized to CP. Like Mitofilin and Casq, MCU and EMRE are enriched in the CP, while prohibitin, another IMM protein, is similarly distributed between CP and IMM. **D.** Immunofluorescence (IF) distribution of MCU and the matrix protein mtHsp 70 in glass-mounted mitochondria (cHM) via 3D super-resolution microscopy (images i-v). mtHsp IF fills the matrix volume while the green MCU-particles are more prevalent (bar chart) at the periphery (inner boundary membrane) than inside (cristae) the volume filled by mtHsp70.

2. Validation of MCU IF in knockout mice.



To isolate mitochondrial labeling, α MCU IF was performed using isolated mitochondria from mouse (control vs. MCU KO) heart that were glued to coverslips and loaded with MTR Red. The number of MCU positive particles per field (upper bar chart) and the mitochondrial area (% of MTR staining) covered by MCU labeling (lower bar chart) were both substantially (by $>90\%$) diminished in the MCU KO sample.

3. Colocalization of MCU and RyR2 in cardiac mitochondrial fractions.

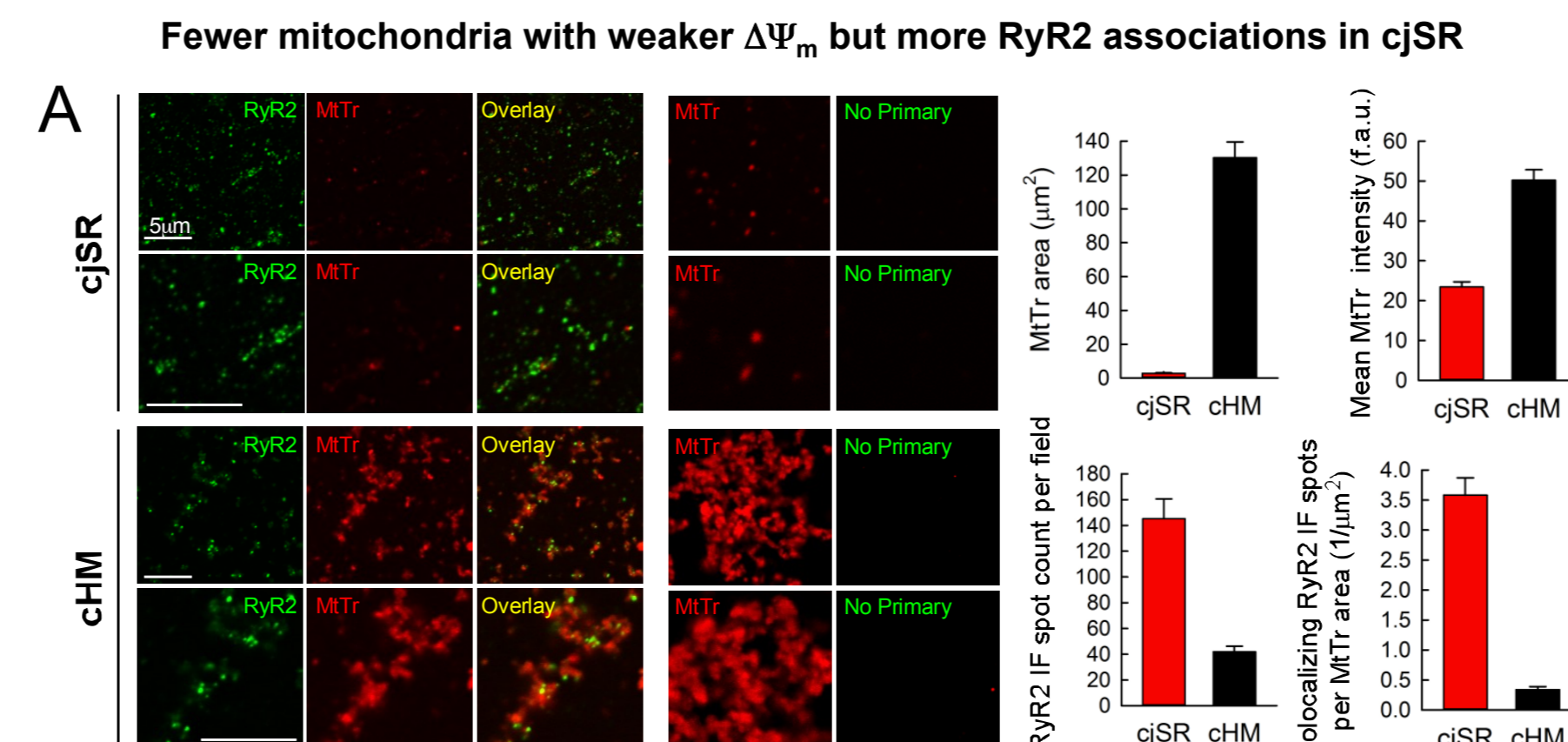


Anti-MCU and anti-RyR2 IF labeling of coverglass-mounted heart mitochondrial fractions (HMTs). **A.** Scheme for the colocalization analysis: top panel shows MCU molecules in a mitochondrion at its transversal side associated with jSR hosting RyR2 clusters. One MCU is at the jSR interface, the other away from it (constellation i). For a mito with equal length and width one transversal side would provide $\sim 17\%$ of the total surface to host MCU. Below are the fluorescent signals emitted by the IF-labeling or MTR, counting with ~ 250 - 300 nm limit in resolution with 2 more possible basic constellations (i, ii, iii). For reference constellation i is also depicted for super-resolution at the bottom. Binarized (threshold) MCU and RyR2 IF spots with overlap were accounted as colocalized (index x; not colocalized \rightarrow nx). The extent of overlap (% of the IF spot area) is shown in yellow. Mean total and colocalizing (% of total) spot counts are shown in the box. **B.** representative image of a close association of a pair of anti-MCU and anti-RyR2 IF clusters resolved by 3D super-resolution microscopy. With the higher resolution (~ 20 - 50 nm) anti-MCU and anti-RyR2 IF are very close but distinct. **C.** Colocalization data from mouse.

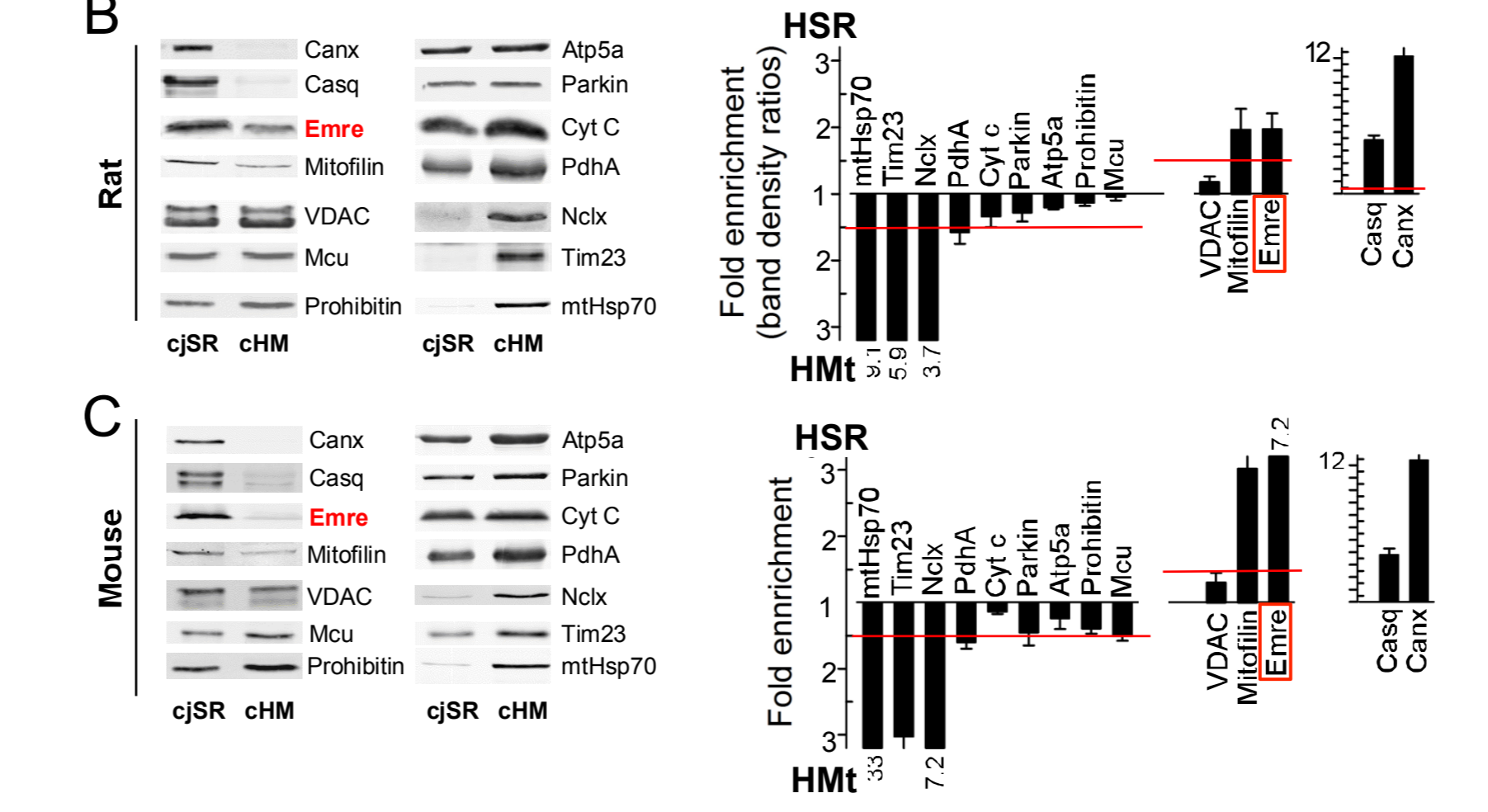
Acknowledgements:

- Grant support: R01 HL122124-01 to GC and SSS
- Grant support: AHA postdoctoral fellowship 16POST27770035 to SF
- High-pressure freezing and freeze-substitution were done in the University of Pennsylvania Electron Microscopy Resource Laboratory core.

4. Comparison of the mitochondrial content in HSR and HMT.

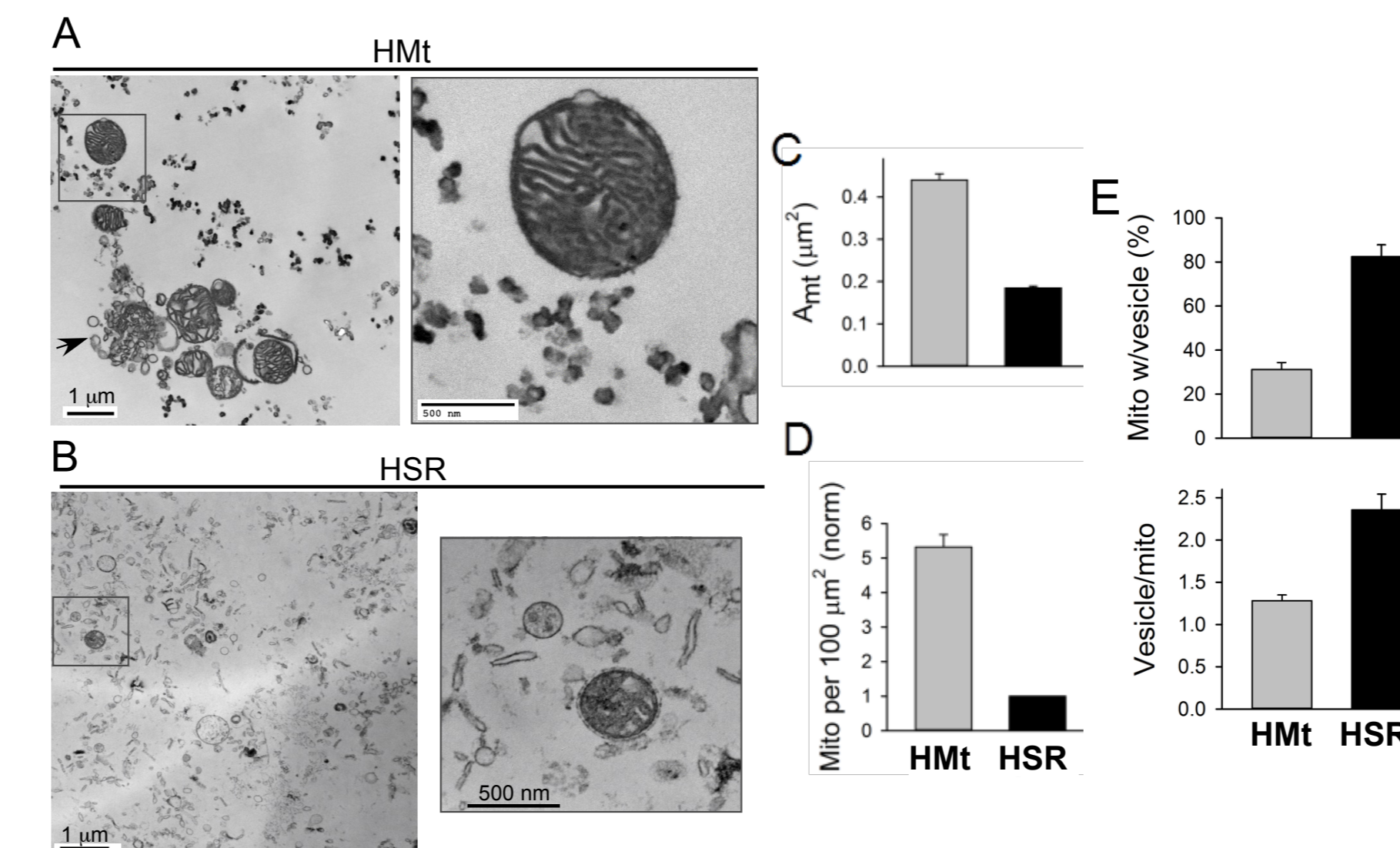


Differing protein profiles



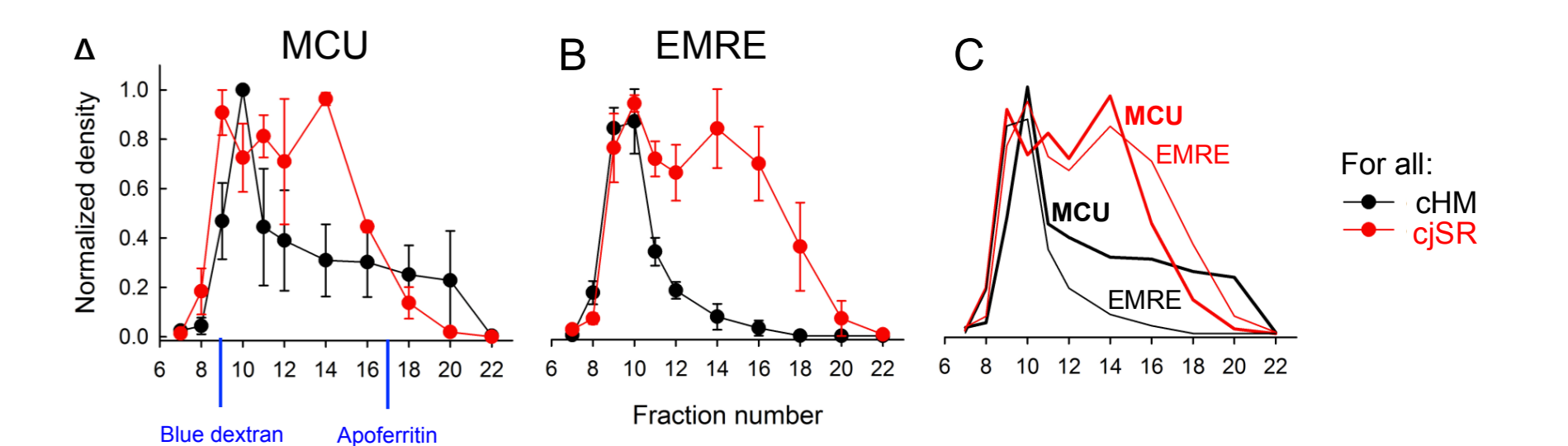
Crude heart SR fraction (HSR, 45,000g post mitochondrial pellet) is frequently "contaminated" with mitochondria or mitochondrial fragments that are small (hence their attachment with SR can significantly decrease their density). If mtCU was biased towards mt-SR associations these mitochondria in HSR would be particularly rich in MCU. **A.** Anti-RyR2 IF and MTRRed distribution in glass-mounted HSR and HMT. Bar graphs show the MTR fluorescence area per field, the mean intensity of MTRRed (loading is $\Delta\Psi_m$ -dependent), the number of RyR2 IF spots per field as well as per area unit of (colocalizing) MTR. While RyR2 spots are <4 fold more numerous in the HSR, the number of colocalizing RyR2 spots per MTR area unit is disproportionately (>10 fold) higher in the HSR. **B.** WBs of various mitochondrial and SR resident proteins in rat HSR and HMT. Bar graphs show the relative enrichment of the respective proteins in the HMT and HSR expressed as fold ratio of the WB band densities. The value of 1 would represent equal band densities between HMT and HSR. Red lines demarcate 1.5 fold enrichment. **C.** Is the same as **B** in mouse.

5. Ultrastructural differences between HSR and HMT



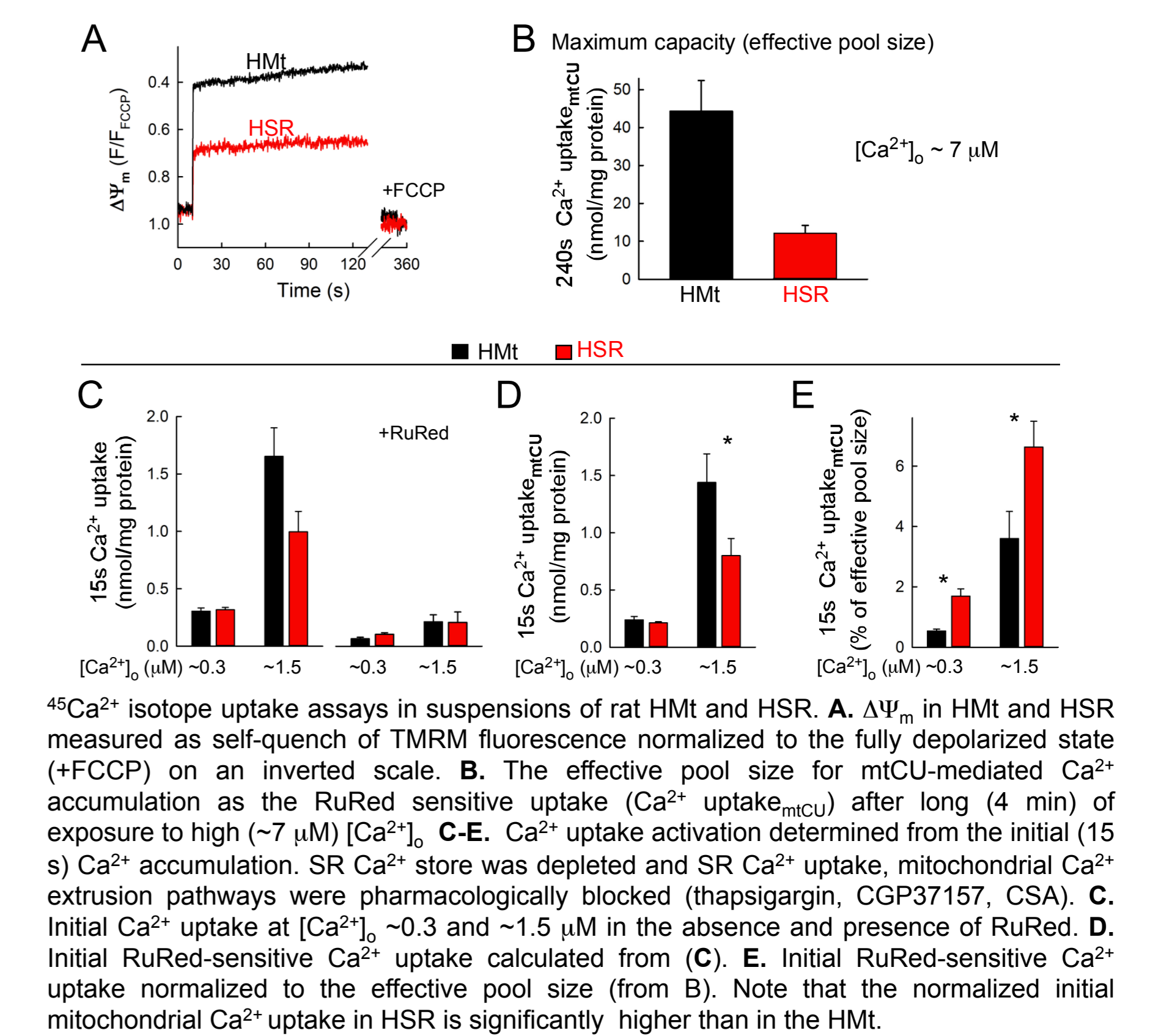
A, B. TEM images of the organelles, membrane vesicles/particles in sections of high-pressure-frozen suspensions of HMT (**A**) and HSR (**B**). The structures are not crammed together as they were not processed as an ultracentrifuge pellet. Bar graphs show the average individual cross-section area (**C**) and quantity (count/100 μm^2) (**D**) of well-defined mitochondria from two independent preparations as well as (**E**) the frequency of mito-vesicle associations along with its extent (vesicle/mito).

6. Size profiles of MCU and EMRE-containing complexes in HMT and HSR



Size-exclusion chromatography profiles of MCU and EMRE from non-denaturing detergent (CHAPS) lysates of HMT (black) and HSR (red). The smaller the fraction number the larger is the size of the complexes. Abundances of MCU (**A**) and EMRE (**B**) proteins in the fractions determined by WB and normalized to the band intensity range. Line plots from **B, C** are overlaid in (**C**). EMRE follows MCU throughout the size range in HSR but not in HMT, where it is un- or underrepresented in the smaller complexes.

7. Greater mitochondrial Ca^{2+} uptake efficacy in HSR than in HMT



CONCLUSIONS

- Tracked by its mandatory constituents MCU and EMRE, the mitochondrial Ca^{2+} uniporter in cardiac muscle concentrates to mitochondrial contact points close to the cytosolic boundary and to interface areas with junctional SR.
- The molecular composition of the mtCU complex (uniplex) is heterogeneous in the cardiac mitochondria. EMRE that is essential for channel function is highly concentrated to jSR associations where it complements all MCU-containing complexes. Outside the mito-jSR association areas smaller MCU-containing complexes are deprived of EMRE, and likely functionally silent.
- mtCU-mediated Ca^{2+} uptake is more effective into the pool of SR-associated small mitochondria and/or mitochondrial segments that sediment in the crude SR (cJSR) fraction than into the larger pool of 'canonical' mitochondria that sediment in the crude mitochondrial fraction (cHM).